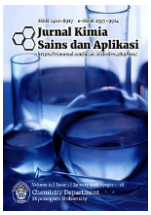
ISSN: 1410-8917
Jurnal Kimia Sains & Aplikasi
e-ISSN: 2597-9914

Jurnal Kimia Sains dan Aplikasi 29 (8) (2026): 568-574

Jurnal Kimia Sains dan Aplikasi
Journal of Scientific and Applied Chemistry

Journal homepage: http://ejournal.undip.ac.id/index.php/ksa



Surface Modification and Kinetic Adsorption of Lampung Natural Zeolite Using Mercapto-Silane: A Study on Ag(I), Cd(II), and Hg(II)

Yulyani Nur Azizah [1,*], Sekar Azzahra [1], Isalmi Aziz [1], Yusraini Dian Inayati Siregar [1], Nurmaya Arofah [2], Ade Saputra [3], Muhammad Al Muttaqii [4]

[1] Department of Chemistry, Faculty of Sciences and Technology, State Islamic University Syarif Hidayatullah Jakarta, Banten, Indonesia
[2] Department of Mining Engineering, Faculty of Sciences and Technology, State Islamic University Syarif Hidayatullah Jakarta, Banten, Indonesia
[3] Research Center for Nuclear Material and Radioactive Waste Technology, National Research and Innovation Agency, Tangerang Selatan, Indonesia
[4] Research Center of Catalysis, National Research and Innovation Agency, Tangerang Selatan, Indonesia

* Corresponding author: yulyani@uinjkt.ac.id

https://doi.org/10.14710/jksa.29.8.568-574

Article Info

Article history:

Received: 04th June 2026
Revised: 30th August 2026
Accepted: 27th September 2026
Online: 30th September 2026

Keywords:
adsorption; functionalization; Lampung natural zeolite; silane; surface modification

Abstract

Heavy metal contamination in water poses serious environmental and health risks due to its toxicity, persistence, and bioaccumulation. This study developed a thiol-functionalized zeolite (ZFT) from activated Lampung natural zeolite via post-treatment silanization using (3-mercaptopropyl)trimethoxysilane for the adsorption of Hg(II), Ag(I), and Cd(II) ions. XRD and FTIR analyses revealed no significant alteration in the clinoptilolite structure following functionalization, with a crystal size range of 10.8–12.80 nm. However, the appearance of a C–H stretching band at 2921 cm^{-1} indicates the presence of organic moieties in the functionalized zeolite, with 3.46 at% S content. Optimum adsorption occurred at pH 4 within 60 min for Hg(II) and Ag(I), and at pH 6 within 100 min for Cd(II), with a maximum tested concentration of 50 mg L^{-1}. Hg(II) adsorption followed the Langmuir isotherm, whereas Ag(I) and Cd(II) fitted the Freundlich model. All adsorption processes followed pseudo-second-order kinetics.

1. Introduction

Heavy metal ion contamination in aquatic environments has become a major global issue requiring proper treatment. Heavy metal pollution originates from both natural sources and anthropogenic activities, such as industrial waste from the galvanizing industry, battery manufacturing, mining, and exhaust gas emissions. Heavy metal ions such as cadmium (Cd) and mercury (Hg) are highly toxic, non-biodegradable, and capable of bioaccumulation in living organisms. Silver (Ag) exposure in excessive amounts may cause argyria, a condition characterized by bluish-gray discoloration of the skin. These heavy metals can damage ecosystems and pose serious risks to human health, including neurological disorders, vital organ damage, and an increased risk of cancer [1]. Therefore, the development of effective, efficient, and environmentally friendly methods for removing heavy metal ions from wastewater is of great importance.

Various methods have been applied for heavy metal treatment, including adsorption, precipitation, neutralization, and ion exchange [2]. Among these methods, adsorption is the most widely used because it is simple, practical, and highly effective for removing heavy metal ions. Heavy metal adsorption can be performed using various adsorbents, including zeolites. An ideal adsorbent should possess high adsorption capacity, good selectivity toward heavy metal ions, and the ability to be regenerated and reused. Zeolite has attracted considerable attention as an adsorbent for removing heavy metal ions from aqueous media owing to its natural abundance and favorable physicochemical properties. Natural zeolite is an aluminosilicate mineral with a porous structure containing well-defined cavities. This unique framework enables zeolite to exhibit adsorption, ion-exchange, and catalytic properties, making it widely applicable in air filtration, wastewater treatment, gas adsorption, fertilizer production, and petrochemical

industries. Its high adsorption capacity and ion-exchange ability make zeolite a promising material for environmental remediation and agricultural applications [3].

Previous studies have demonstrated that thiol-functionalized zeolites exhibit enhanced affinity toward heavy metal ions due to the strong interaction between thiol groups (-SH) as soft bases and heavy metal ions as soft acids such as Ag(I) and Hg(II), consistent with the HSAB (Hard and Soft Acids and Bases) theory. Fardmousavi and Faghihian [4] synthesized thiol-functionalized hierarchical zeolite nanocomposites (SH-Beta/MCM-41) using (3-mercaptopropyl) trimethoxysilane (MPTMS) and achieved a maximum Hg(II) adsorption capacity of 111.11 mg g^{-1}. Similarly, Azizah and Rachman [5] reported that MPTMS modification of Lampung natural zeolite increased the Si/Al ratio and significantly improved heavy metal adsorption while maintaining structural stability. Other studies also confirmed that thiol-containing modifiers enhanced adsorption performance for Pt(II) and Pb(II) ions through improved surface functionality and adsorption kinetics [6, 7].

Despite these advances, most previous studies have focused on adsorbing a single heavy metal ion and have used synthetic or composite zeolites with relatively complex preparation methods. In addition, studies investigating thiol-functionalized Lampung natural zeolite for the simultaneous adsorption behavior of different soft heavy metal ions, particularly Ag(I) and Hg(II), and also Cd (II) as a borderline acid, remain limited. Comparative evaluation of adsorption parameters, adsorption isotherms, and kinetic behavior of these metal ions on a single adsorbent system has not been reported comprehensively. Therefore, further investigation is required to develop a simple, cost-effective, and environmentally friendly thiol-functionalized natural zeolite adsorbent with high selectivity and adsorption performance toward multiple heavy metal ions.

In this study, natural zeolite was activated using NH_4Cl and subsequently functionalized with MPTMS containing thiol groups (-SH) through a silanization method. Structural characterization before and after modification was conducted using X-ray diffraction (XRD), while grafting was analyzed using Fourier-transform infrared (FTIR) spectroscopy and scanning electron microscopy coupled with energy-dispersive X- ray spectroscopy (SEM-EDS). The adsorption performance toward Ag(I), Cd(II), and Hg(II) ions was evaluated by varying pH (2, 4, and 6), contact time (20, 40, 60, and 100 min), and initial metal ion concentration (10–50 mg/L). Atomic Absorption Spectroscopy (AAS) was used to determine adsorption capacity, optimum adsorption conditions, adsorption isotherms, and adsorption kinetics.

2. Experimental

2.1. Materials and Instrumentation

The equipment used in this study included beakers, measuring cylinders, an oven (Memmert), a furnace (NEY Vulcan), a hotplate (Thermo Fisher Scientific), a reflux apparatus, a centrifuge (Hettich EBA 20), X-ray Diffraction (XRD; Shimadzu type 7000), Fourier-Transform Infrared Spectroscopy (FTIR; Bruker-Tenson II), Scanning Electron Microscope with energy-dispersive X-ray spectroscopy (SEM-EDS; Hitachi SU3500) and Atomic Absorption Spectroscopy (AAS; Agilent Technologies).

The materials used were natural zeolite of the clinoptilolite type obtained from CV. Winatama Lampung, (3-mercaptopropyl)trimethoxysilane (MPTMS; Sigma-Aldrich), ammonium chloride (NH_4Cl; Merck), silver nitrate ($AgNO_3$; Merck), mercury(II) chloride ($HgCl_2$; Merck), cadmium sulfate ($CdSO_4$; Merck), distilled water, and ethanol (analytical grade; Merck).

2.2. Methods

2.2.1. Activation and Functionalization of Zeolite

The activation process was carried out by washing the unactivated zeolite (ZA) with deionized water, followed by soaking in 1 M NH_4Cl solution for 24 h at room temperature [8]. The zeolite was then washed repeatedly until chloride-free conditions were achieved and neutralized. Subsequently, the zeolite was calcined at 450°C for 3 h and designated as ZAA.

A total of 2 g of zeolite was dispersed in 100 mL of ethanol–water solution (1:1, v/v) containing 2 mL of MPTMS, followed by refluxing at 80°C for 6 h [9]. The modified zeolite was washed with ethanol and distilled water to remove residual reagents, then dried in an oven at 70°C for 3 h to eliminate moisture. The resulting thiol-functionalized zeolite was designated as ZFT.

2.2.2. Characterization of Crystalline Phase

ZAA and ZFT were characterized by XRD using Cu Kα radiation over the 2θ range 10–90°. Crystal size calculation was performed using the Scherrer equation (1).

$$D = \frac{K\lambda}{\beta \cos\theta} \quad (1)$$

Where, D is the crystallite size (nm), K is the Scherrer constant (0.9), λ is the X-ray wavelength (Cu Kα = 0.15406 nm), β is the full width at half maximum (FWHM) of the diffraction peak in radians, and θ is the Bragg angle, corresponding to half of the diffraction angle (2θ).

2.2.3. Characterization of Functional Group

The ZFT samples were analyzed using an FTIR-ATR instrument over the wavenumber range of 4000–500 cm^{-1} for 45 s at a spectral resolution of 4.0 cm.

2.2.4. Characterization of Morphology and Elemental Analysis

A dried and fine sample was mounted onto conductive carbon tape attached to an SEM stub. SEM images were acquired using a backscattered electron compositional (BSE-COMP) detector at an accelerating voltage of 15 kV, a working distance of 5.9 mm, and a magnification of 3000×. The elemental composition was determined by EDS analysis of representative areas of the samples and reported as weight percentage (wt%) and atomic percentage (at%).

2.2.5. Optimization of Adsorption pH

A total of 100 mg of ZFT was added to 25 mL of Ag(I), Hg(II), and Cd(II) solutions with an initial concentration of 30 mg/L. The mixtures were stirred at 200 rpm for 60 min at varying pH values of 2, 4, and 6. The pH values of 4 and 6 were adjusted using citrate buffer, whereas HCl was used to adjust the pH to 2. After adsorption, the solutions were separated by centrifugation and analyzed using AAS at wavelengths of 228.8 nm for Cd(II), 254 nm for Hg(II), and 328 nm for Ag(I). The adsorption capacity was calculated using Equation (2).

$$Q_e = \frac{((C_o - C_e) \times V)}{m} \quad (2)$$

Where, q_e is the adsorption capacity (mg g^{-1}), C_o and C_e are the initial and final concentration (mg L^{-1}), V is the volume (L), and m is the mass of the adsorbent (g).

2.2.6. Optimization of Contact Time for Adsorption

A total of 100 mg of ZFT was added to 25 mL of metal ion solution with an initial concentration of 30 mg/L. The mixture was stirred at the optimum pH for 20, 40, 60, and 100 min. The adsorption capacity was calculated using Equation (2), as described in the previous section. The relationship between Q_t (the amount of adsorbate adsorbed at time t) and contact time was plotted to determine the adsorption kinetic model based on the highest R^2 value.

2.2.7. Optimization of Initial Metal Ion Concentrations

A total of 100 mg of ZFT was added to 25 mL of metal ion solution with varying concentrations of 10, 20, 30, 40, and 50 mg L^{-1}. The mixtures were stirred under the optimum pH and contact time conditions. The adsorption capacity was calculated using Equation (2), as described previously. For adsorption isotherm analysis, the equilibrium concentration (C_e) and adsorption capacity (q_e) were plotted according to the linear regression equations of the adsorption isotherm models.

3. Results and Discussion

3.1. Characterization of Thiol-Functionalized Zeolite

Zeolite activation was carried out by immersing the material in a 1 M NH_4Cl solution to replace the naturally occurring cations within the zeolite framework with ammonium ions. This treatment enhanced the capacity of the cation exchange and exposed a greater number of active sites on the zeolite surface [8]. Subsequently, the zeolite was functionalized with thiol groups via a silanization reaction using the organosilane MPTMS. The incorporation of thiol groups introduced additional active binding sites, thereby improving the adsorption capability toward the tested metal ions.

The XRD pattern of ZA exhibited several sharp diffraction peaks at 2θ values of approximately 9°, 22°, and 27°, characteristic of clinoptilolite-type zeolite (JCPDS No. 25-1349). After NH_4Cl activation (ZAA), the same characteristic peaks were retained, with slightly increased intensities (Figure 1). This suggests that activation promoted cation exchange while preserving the clinoptilolite framework [10].

Furthermore, the diffraction pattern of the ZFT also displayed the same characteristic peaks as ZA. However, a slight decrease in peak intensity was observed compared with ZAA. This reduction can be attributed to the presence of organic thiol groups from MPTMS attached to the zeolite surface, which partially absorbed the X-ray radiation and reduced the reflected intensity. No significant shift in the 2θ peak positions was detected, indicating that the functionalization process did not alter or damage the crystalline framework of the zeolite [11]. Based on the calculated crystallite sizes, no substantial change was observed throughout the activation and functionalization processes, with the crystallite size remaining within a relatively narrow range of 10.79–12.80 nm.

The surface morphology and elemental composition of the ZFT were investigated using SEM–EDS. The SEM micrograph reveals an irregular, heterogeneous surface morphology characteristic of natural clinoptilolite-containing materials (Figure 2). The EDS analysis confirmed the presence of O, Al, Si, and S in the ZFT sample, with elemental concentrations of 53.81, 5.83, 34.82, and 5.54 wt%, respectively (Table 1). The predominance of O and Si is consistent with the aluminosilicate framework of clinoptilolite, whereas Al is associated with the substitution of Si within the zeolite framework.

The Si/Al atomic ratio calculated from the EDS data is approximately 5.74, which is consistent with the high-silica character expected for clinoptilolite. The sulfur content obtained in this study is also consistent with previously reported SEM–EDX observations for MPTMS-functionalized Lampung natural zeolite (Table 1). Azizah and Rachman [5] reported an S content of 4.75 at% for MPTMS-functionalized Lampung zeolite, together with an increased Si/Al ratio relative to the untreated material [9]. The S content of 3.46 at% obtained for ZFT in the present study, therefore, further supports the successful incorporation of sulfur-containing organosilane species onto the zeolite surface.

Table 1. Elements composition of ZFT

Element	Weight (%)	Atomic (%)
O	53.81	67.38
Al	5.83	4.33
Si	34.82	24.84
S	5.54	3.46

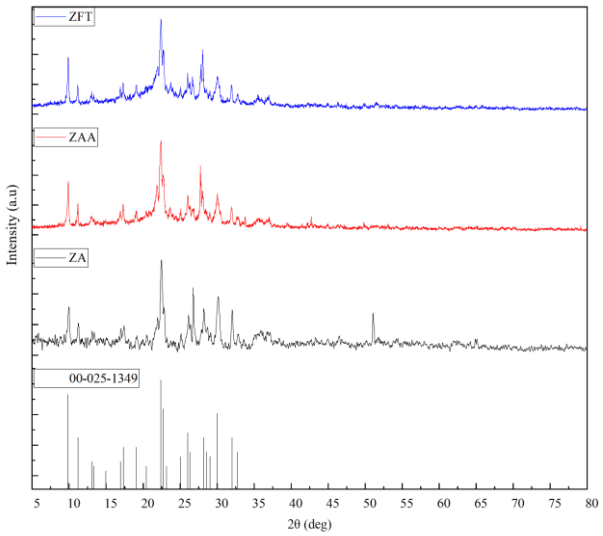


Figure 1. XRD patterns of ZA, ZAA, and ZFT

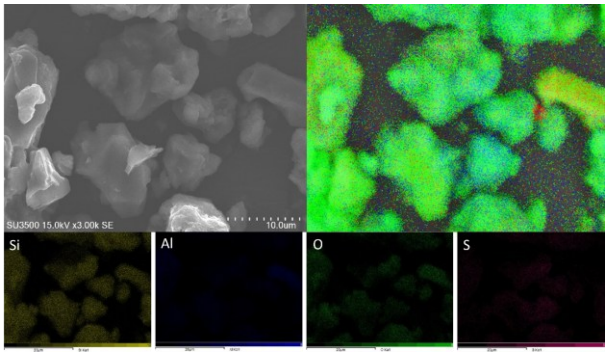


Figure 2. Morphological surface and EDS mapping of ZFT

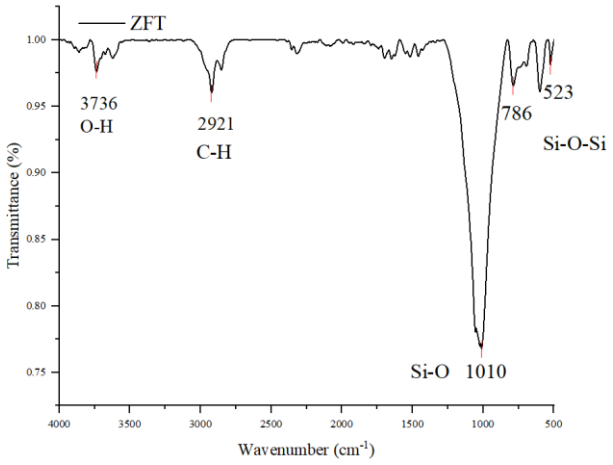


Figure 3. FTIR spectrum of ZFT

FTIR spectroscopy was employed to identify the functional groups present in the zeolite following thiol functionalization. As shown in Figure 3, the FTIR spectrum exhibits a band at 523 cm^{-1}, which can be attributed to the bending vibration of the aluminosilicate framework, while the bands at 786 and 1010 cm^{-1} are associated with the symmetric and asymmetric stretching vibrations of the Si–O–T framework, respectively (T = Si or Al) [12]. A band at 3736 cm^{-1} is assigned to the stretching vibration of O–H groups. However, the characteristic S–H stretching band, typically reported in the region around 2550 cm^{-1}, was not observed in the functionalized zeolite. The absence of this band may be attributed to the relatively low thiol content on the zeolite surface, which may result in an absorption intensity below the detection limit of the FTIR analysis. Nevertheless, the appearance of a band at 2921 cm^{-1}, attributed to C–H stretching vibrations of aliphatic groups [9], provides evidence for the presence of organic species in ZFT. This band was not observed in the spectrum of unmodified natural Lampung zeolite [9], further indicating the introduction of organic groups following the functionalization process.

3.2. Adsorption of Metal Ion

3.2.1. Effect of pH

The effect of pH on adsorption performance was evaluated through experiments using various solution pH conditions. At excessively low pH values, protonation of thiol groups may occur, thereby reducing their ability to bind metal ions. In contrast, excessively high pH values may promote the precipitation of metal ions in the form of metal hydroxides [13]. Therefore, pH optimization is considered an important parameter in determining the adsorption efficiency of each metal ion. The effect of pH on the adsorption capacities of Hg(II), Ag(I), and Cd ions is presented in Figure 4.

The adsorption capacities of all metal ions were relatively high at pH 2 and slightly increased to reach optimum values at pH 4 for Hg(II) and Ag(I) ions. The enhancement in adsorption from pH 2 to pH 4 can be attributed to the reduced competition of H^+ ions for the active –SH sites on zeolite–MPTMS, allowing stronger coordination interactions between sulfur groups and metal ions. At higher pH values, a portion of Hg(II) ions began to form hydroxide precipitates, such as $Hg(OH)_2$, thereby decreasing the availability of free ions for adsorption [13]. Cd exhibited lower affinity toward the – SH functional groups under acidic conditions due to the strong competition from H^+ ions, as well as the borderline character of Cd according to the HSAB principle. At higher pH values (pH 6), a greater number of active sites became available, and Cd remained more stable in its free ionic form, resulting in enhanced adsorption capacity [14].

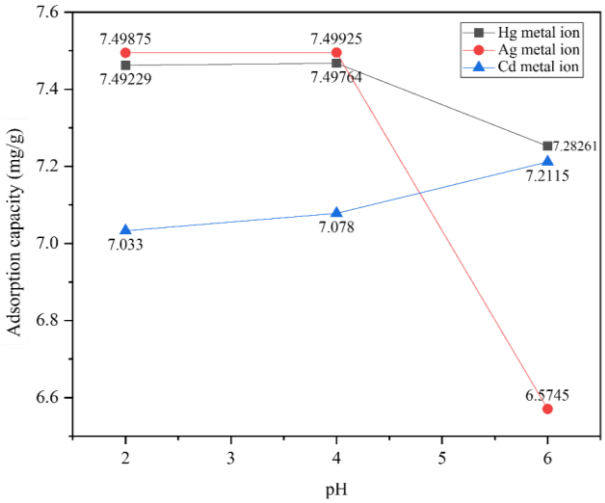


Figure 4. Effect of pH on the adsorption capacity of metal ions

3.2.2. Effect of Contact Time

The contact time variation data showed that the adsorption capacity of metal ions increased gradually, reaching a maximum of 7.47 mg g^{-1} at 60 minutes. This increase indicates that, during the initial stage, many active sites on the ZFT surface were still available, allowing metal ions to readily interact with and bind to the thiol functional groups. After 60 minutes of contact time, the adsorption capacity began to decrease slightly (Figure 5). This condition suggests that the adsorption process had reached equilibrium, where the amount of metal ions adsorbed was nearly equal to the amount released back into the solution. This phenomenon may be attributed to the reduced availability of active sites as well as the possible occurrence of partial desorption due to surface saturation. These findings are consistent with a previous study reported by Waly *et al.* [14], which demonstrated that the adsorption equilibrium of Hg(II) on thiol-functionalized materials was achieved within 60 minutes.

3.2.3. Effect of Concentration

At low concentrations, nearly all metal ions could be effectively adsorbed because the number of available active sites was still sufficient. In contrast, at higher concentrations, the adsorption capacity tended to approach a maximum value due to the limited number of active sites available on the adsorbent surface [15]. This phenomenon indicates a tendency toward saturation conditions on the adsorbent surface. The effect of concentration variation on the adsorption capacities of Hg(II), Ag, and Cd ions is presented in Figure 6.

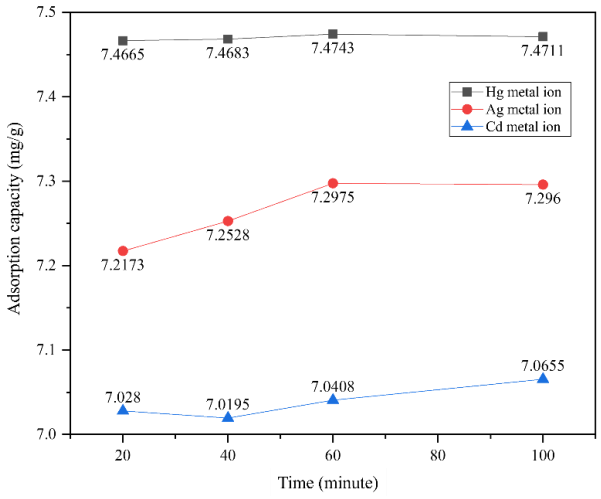


Figure 5. Effect of contact time on the adsorption capacity of metal ions

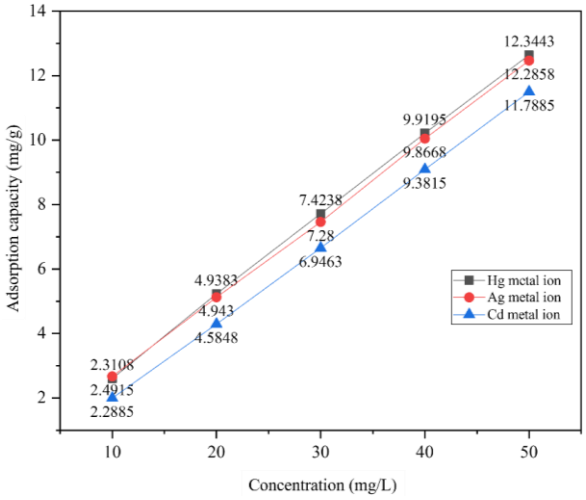


Figure 6. Effect of concentration on the adsorption capacity of metal ions

The experimental results demonstrated that the adsorption capacity (q_e) of metal ions increased with increasing initial solution concentration. At a low concentration of 10 mg L^{-1}, the q_e value was approximately 2.3 mg g^{-1}. This value gradually increased as the solution concentration increased. The adsorption capacity continued to rise to a concentration of 50 mg L^{-1}, at which the q_e value reached 12.3 mg g^{-1}. This trend indicates that the availability of metal ions in the solution plays an important role in determining the amount of ions adsorbed onto the adsorbent surface [16]. Compared with unmodified Lampung natural zeolite, thiol functionalization is expected to enhance the adsorption of soft metal ions, particularly Ag(I) and Hg(II), by introducing sulfur-containing binding sites. According to Zhang *et al.* [17], thiol grafting on zeolite nearly ten-fold increases the adsorption capacity, from 0.041 mmol Hg g^{-1} to 0.445 mmol Hg g^{-1}.

3.3. Adsorption Isotherms

The analysis results showed that the coefficients of determination (R^2) for the Langmuir and the Freundlich isotherm models differed for each metal ion, as presented in Table 2. The results for Ag ions showed that the Freundlich isotherm exhibited a higher R^2 value (0.871) than the Langmuir isotherm (0.769). Similarly, for Cd ions, the Freundlich isotherm yielded a significantly higher R^2 value (0.973) than the Langmuir isotherm (0.844). These findings indicate that the adsorption behavior of Ag and Cd ions is better described by the Freundlich model, suggesting that the adsorption process occurs on a heterogeneous adsorbent surface with non-uniform binding energies [18].

Table 2. Adsorption isotherm of metal ions using the Freundlich and Langmuir models

Isotherm	Parameters	Ag(I)	Cd(II)	Hg(II)
Langmuir	q_{max} (mg g^{-1})	12.28	11.79	12.34
	k_L (L mg^{-1})	6.375	0.15	4.52
	R^2	0.769	0.844	0.598
Freundlich	1/n	0.432	1.328	0.386
	k_F (mg g^{-1})	10.57	2.66	4.499
	R^2	0.871	0.973	0.081

Table 3. Kinetic adsorption analysis of metal ions

Kinetic model	Parameters	Concentration (mgL^{-1})		
		Ag(I)	Hg(II)	Cd(II)
Pseudo-first-order	R^2	0.989	0.998	0.434
	k_1 (min^{-1})	0.051	0.011	0.010
	q_e ($mg\ g^{-1}$)	0.270	0.0095	0.053
Pseudo-second-order	R^2	1	1	1
	k_2 ($g\ mg^{-1}\ min^{-1}$)	0.485	10.53	0.567
	q_e ($mg\ g^{-1}$)	7.321	7.474	7.077

The relatively small difference between the R^2 values indicates that the adsorption of both metal ions still exhibits a tendency to follow the Langmuir model, suggesting that the process is predominantly governed by monolayer formation on specific active sites. The Freundlich constants obtained were k_F = 10.57 for Ag and k_F =2.66 for Cd. This mechanism also allows the occurrence of multilayer adsorption, which is more representative of the actual conditions of complex natural adsorbent surfaces.

3.4. Kinetic Adsorption

The kinetic adsorption analysis of Ag(I), Cd(II), and Hg(II) onto ZFT showed that the pseudo-second-order (PSO) model provided a higher R^2 than the pseudo-first-order (PFO) model (Table 3). The PSO model yielded an R^2 value of 1.000 for all three metal ions, indicating an excellent mathematical fit to the experimental data. However, this perfect fit should be interpreted with caution, as only four contact times (20, 40, 60, and 100 min) were used in the kinetic analysis. The limited number of experimental data points may partly account for the exceptionally high R^2 value and may not fully capture the overall kinetic behavior of the adsorption process. Therefore, although the PSO model provided the best mathematical fit among the models evaluated, the R^2 value alone is insufficient to conclusively determine the underlying adsorption mechanism. Further kinetic studies involving a greater number of contact times, particularly during the initial adsorption stage and near equilibrium, would provide a more robust assessment of the kinetic behavior. Similar findings were reported by Fardmousavi and Faghihian [4], who demonstrated that thiol-functionalized hierarchical zeolite effectively adsorbed Hg(II), with a high adsorption capacity, rapid attainment of equilibrium, and strong agreement with the PSO model ($R^2 > 0.998$).

The thiol functional groups introduced by MPTMS can act as electron-donating sites and interact with metal ions through coordination, particularly with metal ions exhibiting a high affinity for sulfur, such as Hg(II) [19]. The preferential interaction between Hg(II) and sulfur-containing functional groups may contribute to its adsorption behavior, which was better described by the Langmuir isotherm. This result suggests adsorption onto relatively homogeneous sites with comparable binding energies. In contrast, the adsorption of Ag(I) and Cd(II) was better described by the Freundlich isotherm, indicating a heterogeneous distribution of adsorption sites and potentially different interaction energies on the functionalized zeolite surface. These differences, together with the higher PSO rate constant obtained for Hg(II), suggest that the intrinsic characteristics and chemical affinity of the metal ions toward the functionalized surface play important roles in determining the adsorption rate and overall adsorption behavior [20].

4. Conclusion

The chemical activation and surface modification processes applied to Lampung natural zeolite did not alter the clinoptilolite phase or the crystal size, which remained within the range of 10.8–12.8 nm, with a S content of 3.46 at%. The adsorption of Hg(II) and Ag(I) ions reached optimum conditions at pH 4 with a contact time of 60 minutes at a concentration of 50 mg L^{-1}, whereas Cd adsorption was more favorable at pH 6. The adsorption isotherms of Ag and Cd ions were better described by the Freundlich model, indicating a heterogeneous adsorbent surface and the potential for multilayer interactions between the thiol groups on the zeolite surface and the metal ions.

Acknowledgment

The authors acknowledge the facilities and scientific and technical support from the Chemical and Bioprocess Laboratory, National Research and Innovation Agency, through E-Layanan Sains-BRIN.

References

[1] P. B. Tchounwou, C. G. Yedjou, A. K. Patlolla, D. J. Sutton, Heavy Metal Toxicity and the Environment, in: *Molecular, Clinical and Environmental Toxicology*, 2012, https://doi.org/10.1007/978-3-7643-8340-4_6

[2] A. E. Gahrouei, A. Rezapour, M. Pirooz, S. Pourebrahimi, From classic to cutting-edge solutions: A comprehensive review of materials and methods for heavy metal removal from water environments, *Desalination and Water Treatment*, 319, (2024), 100446 https://doi.org/10.1016/j.dwt.2024.100446

[3] M. Senila, O. Cadar, Modification of natural zeolites and their applications for heavy metal removal from polluted environments: Challenges, recent advances, and perspectives, *Heliyon*, 10, 3, (2024), e25303 https://doi.org/10.1016/j.heliyon.2024.e25303

[4] O. Fardmousavi, H. Faghihian, Thiol-functionalized hierarchical zeolite nanocomposite for adsorption of

Hg^{2+} from aqueous solutions, *Comptes Rendus Chimie*, 17, 12, (2014), 1203-1211 https://doi.org/10.1016/j.crci.2014.05.001

[5] Yulyani Nur Azizah, Faizal Rachman, Physico-Chemical Characteristics of Lampung Natural Zeolite Functionalized Mercapto-Silane, *EduChemia (Jurnal Kimia dan Pendidikan)*, 8, 1, (2023), 56-67 https://doi.org/10.30870/educhemia.v8i1.18514

[6] T. Kang, Y. Park, J. Yi, Highly Selective Adsorption of Pt^{2+} and Pd^{2+} Using Thiol-Functionalized Mesoporous Silica, *Industrial & Engineering Chemistry Research*, 43, 6, (2004), 1478-1484 https://doi.org/10.1021/ie030590k

[7] L. P. Sholikah, S. Sumari, Y. D. Yunisari, Modification and Application Study of Activated Natural Zeolite for the Treatment of Liquid Waste from Chemical Laboratory, *Jurnal Kimia Sains dan Aplikasi*, 26, 9, (2023), 332-343 https://doi.org/10.14710/jksa.26.9.332-343

[8] Zaira Adila, Wega Trisunaryanti, Triyono Triyono, Modification of Natural Zeolite from Klaten, Indonesia Using Ammonium Chloride by Ion-Exchange and Its Application as Catalyst in Ethanol Dehydration to Produce Diethyl Ether, *Indonesian Journal of Chemistry*, 24, 2, (2024), 505-518 https://doi.org/10.22146/ijc.90279

[9] Devi Asriani, Pranoto Pranoto, Edi Pramono, Ozi Adi Saputra, Adsorben Berbasis Campuran Andisol/Zeolit/Karbon Aktif untuk Penjernihan Air Gambut, *ALCHEMY Jurnal Penelitian Kimia*, 21, 1, (2025), 138-148 https://doi.org/10.20961/alchemy.21.1.85539.138-148

[10] J. Jiao, J. Sun, R. Ullah, S. Bai, C. Zhai, One-step synthesis of hydrophobic clinoptilolite modified by silanization for the degradation of crystal violet dye in aqueous solution, *RSC Advances*, 10, 38, (2020), 22809-22818 https://doi.org/10.1039/d0ra03151h

[11] Andri Sanjaya, Berliana Putri Agustina, Ageng Kaka Prayoga, Dwinda Salsabila, Jabir Shoji Arhab, Damayanti Damayanti, Wika Atro Auriyani, Yunita Fahni, Desi Riana Saputri, Alkaline Activated Natural Zeolite as a Microbial Immobilization Media in Anaerobic Digestion for Tapioca Wastewater Treatment, *Jurnal Teknologi Lingkungan*, 26, 2, (2025), 173-182 https://doi.org/10.55981/jtl.2025.7432

[12] A. Walcarius, C. Delacôte, Mercury(II) binding to thiol-functionalized mesoporous silicas: Critical effect of pH and sorbent properties on capacity and selectivity, *Analytica Chimica Acta*, 547, 1, (2005), 3-13 https://doi.org/10.1016/j.aca.2004.11.047

[13] Ruiming Song, Zhimei Li, Wanli Li, Ya An, Mei Li, Haoli Qin, Chengshuai Liu, Improved adsorption and desorption behavior of Cd on thiol-modified bentonite grafted with cysteamine hydrochloride, *Research on Chemical Intermediates*, 48, (2022), 2721-2744 https://doi.org/10.1007/s11164-022-04711-y

[14] S. M. Waly, A. M. El-Wakil, W. M. A. El-Maaty, F. S. Awad, Efficient removal of Pb(II) and Hg(II) ions from aqueous solution by amine and thiol modified activated carbon, *Journal of Saudi Chemical Society*, 25, 8, (2021), 101296 https://doi.org/10.1016/j.jscs.2021.101296

[15] Dagang Liu, Zehui Li, Wei Li, Zhengrong Zhong, Jianqiang Xu, Jinjing Ren, Zhongshi Ma, Adsorption Behavior of Heavy Metal Ions from Aqueous Solution by Soy Protein Hollow Microspheres, *Industrial & Engineering Chemistry Research*, 52, 32, (2013), 11036-11044 https://doi.org/10.1021/ie401092f

[16] Ahmed M. Fallataha, Habib Ur Rehman Shah, Khalil Ahmad, Muhammad Ashfaq, Abdul Rauf, Muhammad Muneer, Mohamed M. Ibrahim, Zeinhom M. El-Bahy, Amir Shahzad, Afshain Babras, Rational synthesis and characterization of highly water stable MOF@GO composite for efficient removal of mercury (Hg^{2+}) from water, *Heliyon*, 8, 10, (2022), e10936 https://doi.org/10.1016/j.heliyon.2022.e10936

[17] X. Y. Zhang, Q. C. Wang, S. Q. Zhang, X. J. Sun, Z. S. Zhang, Stabilization/solidification (S/S) of mercury-contaminated hazardous wastes using thiol-functionalized zeolite and Portland cement, *Journal of Hazardous Materials*, 168, 2-3, (2009), 1575-1580 https://doi.org/10.1016/j.jhazmat.2009.03.050

[18] S. D. Miftiyati, S. Hamdiani, M. G. Darmayanti, Paramagnetic Merkapto Silica Hybrid from Rice Husk Ash for Ag(I) Adsorben, *Acta Chimica Asiana*, 1, 2, (2018), 30-36 https://doi.org/10.29303/aca.v1i2.19

[19] T. Velempini, K. Pillay, Sulphur functionalized materials for Hg(II) adsorption: A review, *Journal of Environmental Chemical Engineering*, 7, 5, (2019), 103350 https://doi.org/10.1016/j.jece.2019.103350

[20] M. Benjelloun, Y. Miyah, G. Akdemir Evrendilek, F. Zerrouq, S. Lairini, Recent Advances in Adsorption Kinetic Models: Their Application to Dye Types, *Arabian Journal of Chemistry*, 14, (2021), 202104 https://doi.org/10.1016/j.arabjc.2021.103031